Meso-scale Flight and Miniature Rotorcraft Development

Ilan Kroo, Peter Kunz
Stanford University
Stanford, CA

Abstract

This paper summarizes the initial development of a very small-scale rotorcraft that flies on its own power and carries sensors for atmospheric research or planetary exploration. Initial devices are electrically powered, ranging in size from 2 to 15 cm, and have involved challenges in aerodynamics, control, and manufacturing. Many interesting scaling issues arise as one shrinks a flight vehicle down to this size. Certain scaling attributes are favorable, such as the increased strength and rigidity of structures at small scales, while others, such as aerodynamics, represent significant challenges. This paper summarizes the aerodynamic design of the rotor system, and approaches to fabrication, control, and power systems. Results of prototype tests suggest that the concept can be successfully produced and that the design methodology is appropriate, despite the insect-like scale of the rotors. Results of recent experiments with a larger version of this concept intended to fly on Mars are also described.

Introduction

The rapid development of microelectronics and microelectromechanical systems (MEMS) has made it possible to incorporate a variety of computing, communications, and sensing functions on air vehicles with masses of less than 100g. Micro air vehicles (MAVs) with 15 cm spans are now flying with realtime video, GPS, and sophisticated autopilot functions. With the idea that progress in these areas will continue, we have looked at what might be possible for future MAVs, focusing on airframe technologies that would enable flight at even smaller scales.

Such vehicles would have many unique capabilities including the ability to fly indoors or in swarms to provide sensor information over a wide area at a specific time. The very low mass of these devices might make them attractive for planetary exploration, of Mars or Titan for example, due to the high cost of transporting each gram [1]. Although sub-gram imaging systems are not available, miniature aerial robots might be used in the near term for simple atmospheric sensing tasks.

Our investigation focuses on meso-scale systems – devices larger than microscopic, yet significantly smaller than conventional air vehicles. Such rotorcraft, termed mesicopters, are centimeter-scale devices with masses of 3 to 15g, powered by DC motors (figure 1). To achieve this goal, the program has begun with the development of somewhat larger vehicles with masses up to 60g. This provides near-term payload capabilities while reducing the cost of the development program.

Hovering vs. Forward Flight

That fixed wing aircraft dominate aeronautical development may be attributed to two factors. First, aircraft have generally been employed for transportation of people or goods. The goal is not just to remain airborne, but to get from point A to point B. Not all applications require the high speed capability of aircraft, but this has been an obvious feature to exploit. Although surveillance, communications, and imaging (information-related) applications have existed for some time, only recently has this started to become possible with very low mass systems. Second, and most importantly, hovering requires substantially more power than does forward flight – at least for conventionally-sized systems. Even if the rotor and wing dimensions are similar, the aircraft in forward flight requires a thrust of W / L/D to maintain level flight, while the rotor requires a thrust equal to the vehicle weight. However, the required power for a fixed wing airplane increases with speed when the thrust is given. So if the wing L/D is small and the speed that would be required to sustain flight is large, the discrepancy between the required power for forward flight and hover is less significant. In some cases, especially at very low Reynolds numbers, the two flight modes require very similar power inputs. This can be seen more quantitatively as follows:

The power required by a fixed wing aircraft to maintain level flight is:

$$P = TV / \eta_p = W / L/D \, (2W / S\rho C_L)^{1/2} / \eta_p$$

where: T is the thrust, V the forward speed, η_p the propeller efficiency, W the weight, S the wing area, and C_L the wing lift coefficient.

The power required for hover is:

$$P = T \, V_h / M = W \, (W / 2S\rho)^{1/2} / M$$

where: V_h is the induced velocity in hover and M is the rotor figure of merit.

If we compare the power required for hover with that required for level flight of a propeller-powered fixed wing aircraft: $P' = (P/W)_{hover} / (P/W)_{fixed}$

$$= L/D \, \eta_p (W / 2S\rho)^{1/2} / M(2W / S\rho C_L)^{1/2}$$

Now if, just for comparison purposes, we set the disk loading equal to the wing loading and operate the vehicles at the same density:

$$P' = L/D \, (C_L / 4)^{1/2} \, \eta_p / M$$

So the difference between rotorcraft and fixed wing aircraft is diminished as the L/D and C_L of the fixed wing vehicle become small, as in the case of low Reynolds number flight. If we consider a 15cm span MAV with a L/D of 5 at a C_L of 0.2 (and assume, arguably, that the rotor figure of merit and propeller efficiency are similar), a hovering vehicle would require only 12% more power than the fixed wing device. For larger aircraft this is not at all the case. For a HAE UAV with L/D = 35 and C_L=1.0 the power ratio is 17.5. Of course, the fixed wing MAV flies forward at rather

high speeds, while the rotorcraft hovers. This may be an advantage or disadvantage, depending on the intended mission, but the point is that at these scales the often-assumed efficiency disadvantage of rotorcraft is not apparent. As the scale is further reduced, and the L/D and optimal C_L of the fixed wing airplane are further reduced, the comparison is even more favorable. Furthermore, the rotor weight for a given disk area may be significantly lower than that of a similarly-sized wing together with a propeller and tail surfaces.

Rotorcraft may also be desirable for certain missions because of their compact form factor and ability to maintain their position in hover. In many imaging applications, the conventional aircraft's minimum speed limitations are problematic. Current designs for a Mars aircraft indicate that to avoid excessive vehicle dimensions, flight speeds of Mach 0.5 to 0.6 are required, limiting low altitude, high-resolution imaging options. Finally, with a rotorcraft design of this size we can provide sufficient control for a four-rotor vehicle using motor speed control, avoiding problems with control surface aerodynamics and actuation that plague small aircraft of conventional design.

Rotating vs. Flapping

It has been noted that the only truly successful examples of flight at such small scales are insects, which achieve flight using wing flapping, rather than rotary motion. Indeed Ellington[2], Dickinson[3], and others have argued that unsteady aerodynamic effects may be significant features of insect flight, increasing the achievable maximum lift at very low Reynolds numbers. A number of successful powered ornithopters have been developed and, despite the fact that these have generally achieved poor efficiencies, there is little question that the approach can be used. It is most attractive at small scales where inertial loads do not dominate and where unsteady phenomena may be helpful. Still, the complexity of the flow field, the required wing motion, and the mechanism itself leads one first to ask not whether a flapping device can be used, but whether it must be used. Just as automobiles depart from the paradigm suggested by walking animals, we have started by considering the simple steady motion of a rotor, eliminating mechanical complexity and simplifying stability and control issues. Rotary motion does not preclude the possibility of exploiting unsteady effects and we are currently considering the potential for increased maximum lift with rotor speed modulation.

Fundamental Scaling Issues

The obvious success of small flying animals, in fact the absence of very large flying animals, suggests that flight at very small scales may be more easily accomplished than flight at larger scales. Some of the relevant scaling laws (e.g. increased strength and stiffness with smaller size) have a beneficial effect on the design of small flight vehicles, while others (e.g. aerodynamics) make the design of small-scale aircraft more difficult. Tennekes[4] shows that the wing loading (W/S) of flying devices increases with size. While this result is likely related to various versions of a square-cubed law, it is surely more complicated than the simple constant density scaling suggested in this reference. One part of the explanation for this trend in nature is that smaller, lighter creatures can more feasibly contend with relatively larger wings because of improved structural properties (strength and stiffness / weight) at small scales. This is also a feature that can be exploited with a small rotorcraft. Rotor weight and aeroelasticity are not problems for tiny rotors with a disk loading of less than 25 N/m^2 (0.5 lb/ft^2), while large helicopters have disk

loadings of 500 N/m^2 (10 lb/ft^2) or more and would become unmanageable with rotors 4 to 5 times as large. The lower attainable disk loading is one favorable attribute of small rotorcraft since the *required* power-to-weight ratio scales as the square root of the disk loading.

The *available* power-to-weight ratio depends on the motor and power source. While scaling of devices such as gas turbines may be quite different from permanent magnet motors, out initial devices consist of electrically driven rotors with energy stored in batteries. Available small DC motors show relatively little effect of size on their power-to-weight ratio, although the efficiencies of the very small motors are usually smaller than larger versions. The specific energy of batteries depends more on chemistry than size, although very small batteries are often dominated by case weight. A study of commercial DC motors and batteries suggested that scaling effects on available power-to-weight ratio were not significant over the 4-5 orders of magnitude considered. See figures 2, 3. If it were not for Reynolds number effects, a miniature electric rotorcraft would have some fundamental advantages over larger devices since the required power-to-weight ratio is reduced by low disk loading, while the available power-to-weight is little changed with size.

The reduction of Reynolds number with vehicle size poses one of the greatest challenges for meso-scale flight. While section lift-to-drag ratios of 200 and above are common for large airfoils, the increased skin friction at small scales leads to values in the range of 5 to 15 for Reynolds numbers in the thousands. (Figure 4.)

Approach

The development of the meso-scale rotorcraft is ongoing and has involved challenges in many disciplines. Some of the primary issues are summarized below.

Insect-Scale Aerodynamics: The Reynolds number of the mesicopter rotors lies in the range of 1,000 to 6,000 where aerodynamics are dominated by viscous considerations and few design tools are available. This is one of the areas in which scaling laws are unfavorable, with lower lift-to-drag ratios and limited rotor lift capabilities. Some of the aerodynamic features are poorly understood in this size regime and means by which improved performance may be realized have been little explored. Because the flow is viscous, some of the simpler tools used for propeller and rotor design are not applicable and basic design rules (e.g. nearly constant inflow) are not appropriate.

3-D Micro-Manufacturing: To achieve high lift-to-drag ratios smooth rotors with 3D surfaces at micro scale dimensions must be built. Traditional micro- fabrication techniques can generate features at and below the desired size scales. Yet the need to produce smooth 3D surface features requires rethinking processing steps commonly used for the building of IC and MEMS structures. Traditional 3D machining methods are not normally employed for the fabrication of parts and devices as thin as 50microns, yet their resolution of a few microns makes them attractive candidates for shaping surfaces within this size regime.

Integration of Power and Control Systems: Although many types of batteries with high specific energy are becoming available, identifying very small batteries suitable for the Mesicopter, with good specific energy and high current rates is not easy. The control of these small devices is also a problem. Because of their size, stability time constants are very short and the mass budget for motor/flight control sensors and processing is limited.

The basic approach has been to develop scalable design and fabrication methods and to start with devices that are larger than the eventual goal. The (super) scale model prototypes are sufficiently large that commercial motors, batteries, and electronics can be employed. The first such prototype is shown in figure 5 with a maximum takeoff weight of about 3g. This device was used to gather data on aerodynamic performance and required an external power supply since the planned Li-Ion batteries were not yet available. A second prototype with a maximum weight of 10-15g is currently being tested and can utilize existing batteries. Finally, a stability and control testbed with even larger dimensions and with a mass of 60g is also under development. As these systems are refined, the scale will be reduced to explore the limits of this technology.

Aerodynamic Design

The operating regime of the meso-scale helicopter poses difficulties for aerodynamic analysis and design. Current sizing and motor parameters result in a rotor tip Reynolds number of approximately 5000. Little experimental or computation work has been published on aerodynamic lifting surfaces operating at such low Reynolds numbers (cf. [5]) and it is unclear to what extent classical airfoil and rotor analysis and design methods are applicable in this flow regime. The highly viscous nature of the flow field, large increases in the boundary layer thickness, and the potential for large regions of separated flow, create the potential for large discrepancies in performance from what might be expected based on experience at higher Reynolds numbers. The present approach involves a simplified 3-D rotor analysis and optimization code, coupled with more complete 2-D rotor section analysis. Results from the viscous section analyses are combined with the 3-D design code using regression-based models of the 2-D results. Although this approach is similar to that used for larger scale rotorcraft design, the successful implementation of the approach was not straightforward and some surprising results were obtained.

2-D Analysis and Design

It has been suggested that at such low Reynolds numbers airfoil geometry is not important and that most any inclined plate is as good as an airfoil section. Our initial looks at section performance using the Navier-Stokes solver INS2D [6] indicated that this was not correct. In addition to important effects of thickness (as shown in figure 4), details of the section edge shape are significant as is the camber distribution. Figure 6 shows a sample result from the CFD computation, illustrating the very thick “boundary layer” and the effect of Reynolds number and thickness form on section drag polars. The large influence of viscosity on the section pressure distribution changes some of the usual approaches to airfoil design. These considerations are

described further in a companion paper [7] on airfoil design for the mesicopter, including the numerical optimization of section camber which leads to the geometry shown in figure 7.

3-D Design

The 3-D rotor design was based on classical blade element methods with inflow computed using momentum and vortex theory [8]. The analysis incorporates viscous effects in several ways, including an estimate of the swirl introduced by blade profile drag. This simple method was reasonably successful in predicting the rotor performance in hover, but an improved analysis using 3D Navier-Stokes modeling is currently underway.

Since the blade l/d is low and since l/d and C_{lmax} depend strongly on Reynolds number, some of the simpler approaches to design (e.g. minimum induced loss concepts) lead to less than optimal solutions. Nonlinear optimization was therefore employed to determine the blade chord and twist distribution along with rotor diameter and RPM. Models of the section drag polars were constructed from the Navier-Stokes computations and motor performance models, based on tests of the brushless DC motors, were incorporated directly in the optimization. Optimization results for the larger device show that the rotor is more strongly constrained by maximum solidity. The second prototype requires approximately four times the lift on each rotor and is constrained to 2.2 cm rotor diameter if ungeared commercial DC motors are used. This leads to the geometry shown on the right of figure 8.

Rotor Fabrication

One of the more challenging aspects of creating an efficient mesicopter is the fabrication of the rotor. The optimally designed blades are very thin 3-dimensional structures, with minimum strength and stiffness properties for operation and handling. For the 1.5cm rotors significant aerodynamic performance penalties were predicted for thicknesses in excess of 50 μm. Three material categories were considered -- polymers, metals, and ceramics -- and a variety of manufacturing processes for these material categories were explored. The process selected and implemented by Stanford's Rapid Prototyping Laboratory is known as Shape Deposition Manufacturing, a sequence of additive and subtractive processing steps for the fabrication of complex 3D parts. Mold SDM is a variation of this process for the creation of complex shaped fugitive wax molds. A spectrum of castable polymer and ceramic materials have been used to make parts from these molds. [9]

The sequence of manufacturing steps is illustrated in figure 9 and involves the following:

- *CAD modeling based on the design parameters:* Chord length, twist angle and cross-section shapes are given at several stations along the radius. Due to the manufacturing and strength considerations, the parts close to the center hub are modified to avoid weak connections and stress concentrations.
- *CNC code generation:* After the model is created, CNC machining code is generated using a commercial CAD/CAM package.
- *Substrate preparation:* Support material is machined to obtain the geometry of bottom surface

of rotor by 3-axis CNC mill. (step 1)
• *Polymer casting*. Part material, i.e. polymer, is cast to fill cavity. (step 2)
• *Surface flattening:* Excess polymer on top of the wax surface is removed. (step 3)
• *Material shaping to net shape*. CNC machine geometry of top rotor surface. (step 4)
• *Substrate removal*. If the rotors cannot be pulled out of the substrate directly, wax is melted at 150 degrees C, remaining traces can be removed with BioAct. (step 5)

Rotor testing revealed that the actual thrust produced was less than that predicted by the aerodynamic analysis. While the aerodynamic approximations made in the interest of reasonable computation times might account for this, it is also possible that the as-built parts did not conform to the intended design. To verify this, detailed studies of the rotor shape were conducted using scanning electron microscopy and laser validation of the actual rotor. An example image of the section shape at 75% of the rotor radius is shown in figure 10. On the right side of the figure, optical sensing shows significant discrepancies in the as-built incidence. This was corrected by using a wax substrate with lower melting temperatures for subsequent rotors.

In fact, the rotor section shapes did not well approximate the initially designed sections as the desired thicknesses dropped considerably below the minimum 50 μm that could be machined using this process. Subsequent CFD analysis showed that while maintaining small maximum thickness was important to good aerodynamic performance, sections with more uniform thickness distributions were acceptable.

Power Systems
Initial prototypes use commercially available brushless DC motors (made by RMB in Switzerland). These motors achieve very high efficiencies (60%-67%) for their small size (mass as low as 325mg). Of course brushless motors require motor control electronics and to achieve the rated power and efficiency, rather sophisticated closed-loop controllers are required. The motor manufacturer sells a closed loop controller, but this weighs hundreds of grams. For this project, the control electronics have been replicated using small components with a total weight of much less than 1g. A more difficult problem is associated with the voltage requirements for the motors and controllers. Since an input of 4-9 volts is required, a rather large number of cells is necessary to drive the motors, using NiCd or AgO_2 chemistries. Lithium batteries are a natural choice, but small, high current lithiums are not available in the sizes required. Stanford and SRI researchers have explored new lithium polymer technologies that will eventually provide an ideal power source for these devices, but this system is still evolving and is not currently available for the Mesicopter prototypes. A more convenient approach involves the use of fewer cells (perhaps as few as 1) and a voltage multiplier to achieve the required voltage levels for the available motors. This is our current approach for the smaller devices and electronics development is proceeding in parallel with the system testing.

Control

The basic concept of the 4-rotor design is that vehicle control can be achieved using the motor controllers described in the previous section. This is convenient as it requires no additional electronics and avoids problems associated with additional actuators. By varying the torque applied to the four motors one can achieve roll, pitch, and yaw control, and overall thrust. This strategy for control is not feasible for large rotorcraft, but because of their small size, the mesicopter rotor inertia is very low and the control bandwidth is high. Such configurations have been flown on a larger scale and several successful hobby models achieve stable controllable flight with some additional damping provided by gyro-based feedback.

To determine if the configuration could be made passively stable or to design gains that would be required, a linear model of the rotor aerodynamics was developed and combined with a nonlinear simulation of the vehicle dynamics. This analysis suggested that the vehicle was unstable, but could be stabilized with a moderate amount of rate feedback from a MEMS gyro. Subsequent studies showed that by carefully positioning the center of gravity and canting the thrustline inward, natural stability might be achieved. Figure 11 shows the results of this analysis in the form of a root-locus diagram. The figure indicates that certain combinations of vertical c.g. position and rotor cant angle produce well-damped designs. Whether this is sufficient for commanded control of the vehicles is being addressed with the development of a stability and control testbed. This 60g rotorcraft flies using commercial lithium-ion batteries and is commanded using a conventional pulse-width modulated signal from an R/C transmitter.

Sensors

Work on performance and stability has remained the focus of this research to date. One of the next areas for study includes possible sensors for improved flight control. While rate gyros may be used to provide stability augmentation, very small scale magnetometers and air data systems have been developed for DARPA's MAV program and may be integrated into these devices at some point. Even extremely small scale GPS is a possibility. New concepts for centimeter-level position sensing using carrier-phase differential GPS with a flight system weight of order 1g are currently being considered. Less exotic sensors, including imaging systems, can more easily be incorporated on the stability and control testbed and this is planned in the next few months.

Testing

The testing program to date has included motor, battery, and controller characterization, rotor testing to determine thrust and torque, and complete 4-rotor constrained vehicle tests. Figure 12 shows initial single rotor and 4-rotor tests on a pivoted arm that constrained the motion to a single degree of freedom before stability and control issues were addressed. This approach has been superceded by more accurate force and moment tests on a test stand constructed for this purpose.

Results of these tests suggested that the aerodynamic design approach was appropriate at this scale, with maximum thrusts of about 80% of the predicted values, despite departures from the assumed section shape. Rotors for the larger prototype have also been fabricated and tested, but show substantially less lift than predicted. This has been attributed to differences between the designed and as-built geometries, although more significant 3D viscous effects (e.g. viscous-induced swirl) than have been modeled remains a possibility under current study.

Initial tests of a miniature rotorcraft designed to fly in the Martian atmosphere have recently been completed in collaboration with researchers at JPL. The basic configuration is similar to the other mesicopter designs, but due to the very low atmospheric density and the desire to carry payloads of at least 10g, the required rotor size was 10 times as large. In addition, the Reynolds numbers are even smaller than for the 1.5cm diameter mesicopter, ranging from 1,000 to 2,000. A very lightweight carbon blade was fabricated and tested in a Mars atmosphere simulation chamber at JPL. A view of the test from the observation window and an image of the rotor are shown in figure 13. The rotor did produce lift despite the near vacuum conditions, but like the previous high solidity design, the lift produced was somewhat less than predicted based on the simple 3D model. Additional design studies and rotor analyses are planned for this application and related missions such as described in [1].

Conclusions and Future Work

A set of analysis, design, and fabrication methods has been applied to investigate the feasibility of very small rotorcraft. Studies have included a range of vehicle sizes and suggest that mesicopters as small as 1.5 cm are possible, while devices that can carry 10g of payload may be

more easily realized and are of greater current interest. These devices may be used in the near future to carry very simple sensors and may, in the more distant future, be controlled in groups that can provide unique information gathering capabilities.

Continuing work in three dimensional, low Reynolds number aerodynamics will be pursued in parallel with a focused effort on stability, control, and communication. Free flights of our prototypes are imminent. These prototypes will provide an excellent testbed for work on distributed control concepts, aerodynamics, and miniature systems development.

Acknowledgements

This work was supported by the NASA Institute for Advanced Concepts, established by the Universities Space Research Association, and funded by NASA. This work is a partnership between the Aeronautics and Astronautics Department and the Mechanical Engineering Department at Stanford. Prof. Fritz Prinz leads the fabrication aspects of the project and directs the Rapid Prototyping Lab where the mesicopters are built. Important aspects of this work were accomplished by doctoral students in Aero/Astro and M.E., while researchers at NASA Ames, Langley, and JPL have provided much appreciated technical assistance.

References

1. Young, L., et al., "Design Opportuinties and Challenges in the Development of Vertical Lift Planetary Aerial Vehicles," presented at the American Helicopter Society International Vertical Lift Aircraft Design Specialists' Meeting, San Francisco, CA, Jan. 2000.

2. Ellington, C.P., *Philos. Trans. R. Soc. Lond.* Ser. B 305, 145, 1984.

3. Dickinson, M.H., Lehmann, F.O., Sane, S.P., "Wing Rotation and the Aerodynamic Basis of Insect Flight," *Science* Vol. 284 No. 5422, June 1999.

4. Tennekes, H., *The Simple Science of Flight*, M.I.T. Press, 1997.

5. N. Miki, I Shimoyama, "Analysis of the Flight Performance of Small Magnetic Rotating Wings for Use in Microrobots", Proc. 1998 IEEE International Conf. on Robotics and Automation, Leuven, Belgium, May 1998.

6. Rogers, S. E., Kwak, D., "An Upwind Differencing Scheme for the Time Accurate Incompressible Navier-Stokes Equations," AIAA Paper 88-2583, June 1988.

7. Kunz, P., Kroo, I., "Analysis, Design, and Testing of Airfoils for Use at Ultra-Low Reynolds Numbers," Conference on Fixed, Flapping, and Rotary Wing Vehicles at Very Low Reynolds Numbers, Notre Dame, June 2000.

8. Johnson, W., Helicopter Theory, Princeton University Press, New Jersey, 1980

9. A.G. Cooper, S. Kang, J. W. Kietzman, F. B. Prinz, J. L. Lombardi and L. Weiss, "Automated Fabrication of Complex Molded Parts Using Mold SDM" (PDF, 205k), *Proceedings of the Solid Freeform Fabrication Symposium*, University of Texas at Austin, Austin, Texas, August 1998.

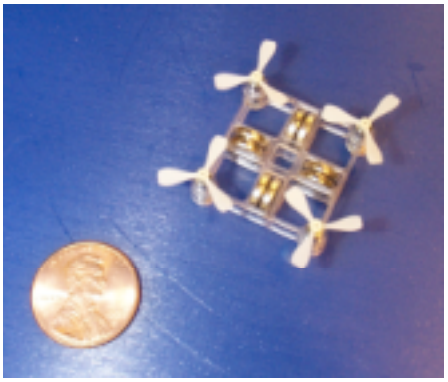

Figure 1. The mesicopter: a meso-scale flying device.

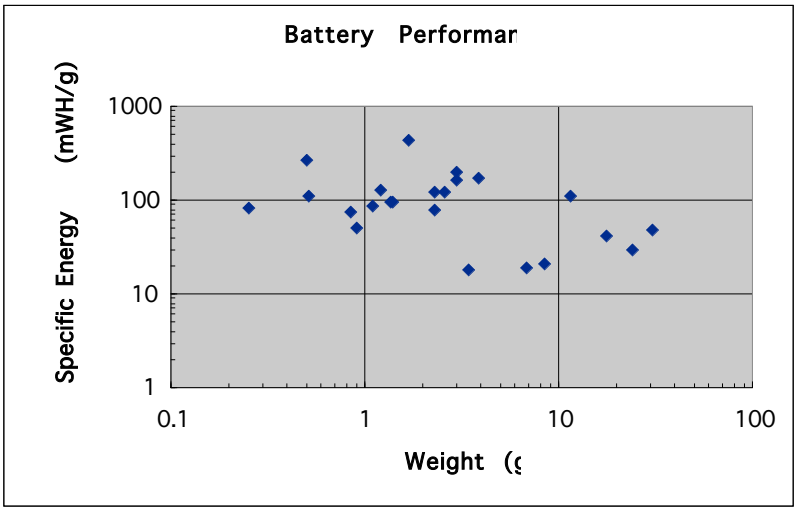

Figure 2. Note that this is specific energy or specific power for a given required endurance. Some of the batteries here have power output limitations that make them unsuitable. Plot includes several chemistries.

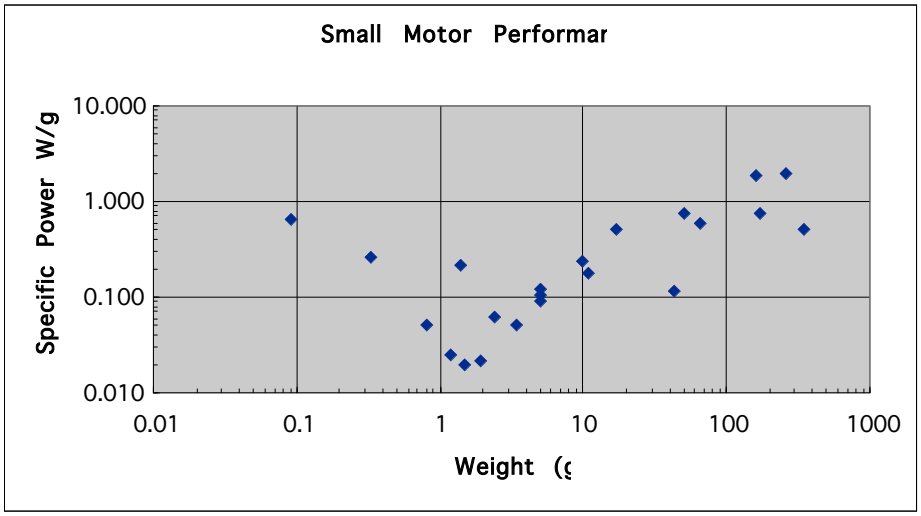

Figure 3. Specific power of several commercially available DC motors. Efficiency varies and motors include brushed, coreless, and brushless configurations.

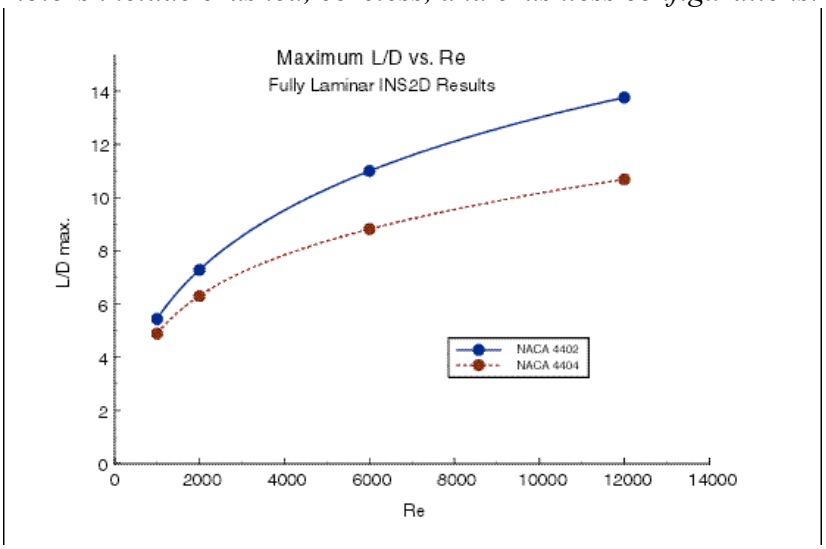

Figure 4. Reduction in section L/D with Reynolds number. Note importance of section thickness.

Figure 5. Initial prototype

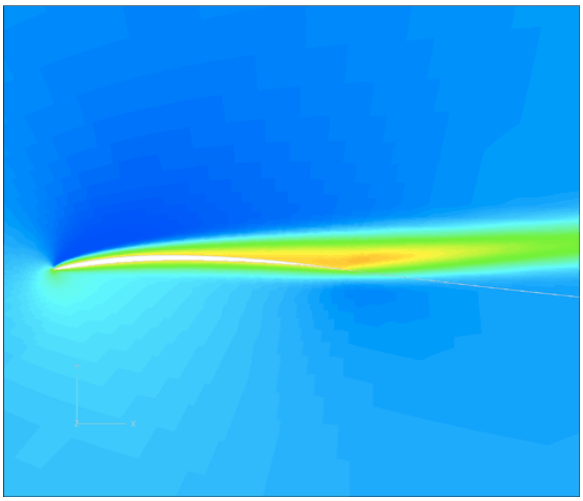

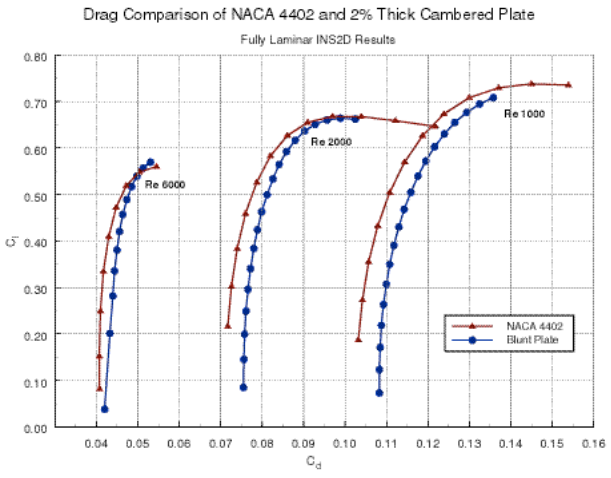

Figure 6. CFD results. Left: contours of constant total pressure illustrate thick boundary layer flow at these conditions. (Re = 5000, □ = 8deg). Right: NACA and 2% cambered plate polars.

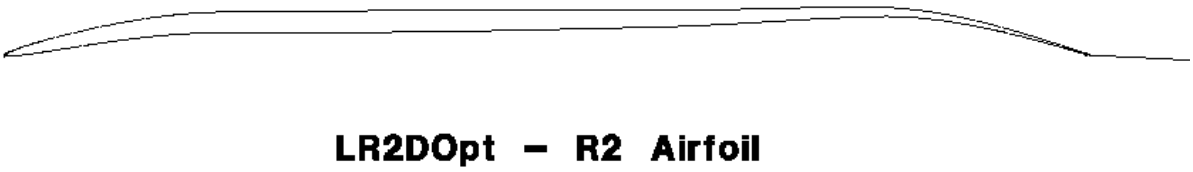

Figure 7. Airfoil optimized for maximum L/D at a Reynolds number of 6000.

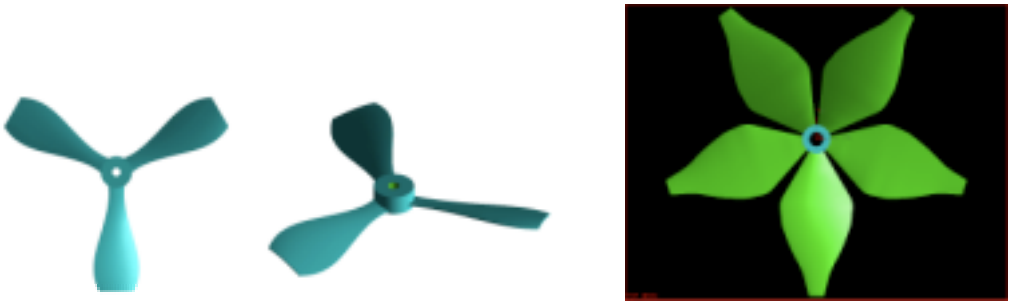

Figure 8. Optimized blade geometries differ greatly due to different motor characteristics. On left: 1.5cm rotors. On right: 2.2 cm rotors designed for four times the thrust.

Figure 9. Steps in rotor fabrication

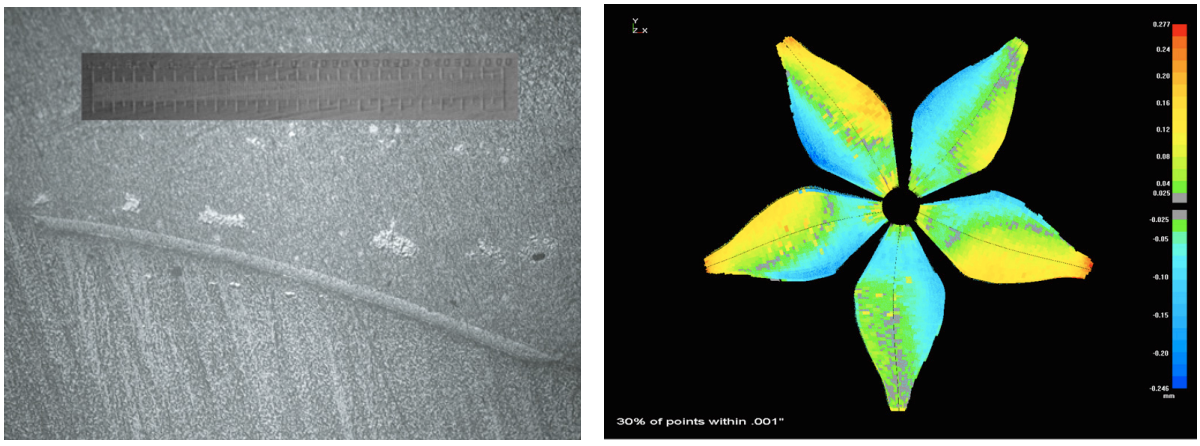

Figure 10. Left: SEM image of section shape at 0.75R. Chord is approximately 3mm. Right: Laser scanning measurements showing error in as-built geometry.

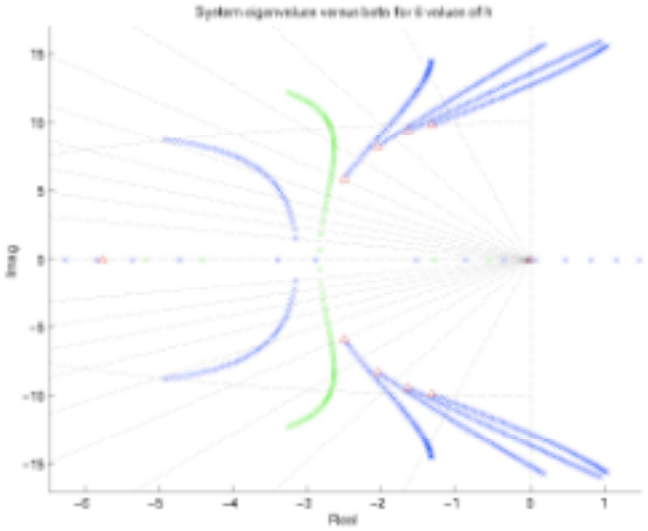

Figure 11. Roots of linearized mesicopter characteristic equations of motion vs. vertical c.g. position and rotor cant angle.

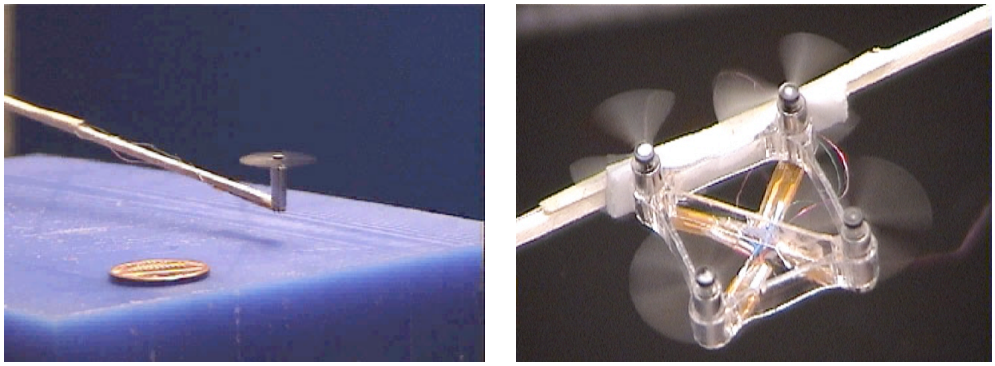

Figure 12. Initial single rotor and 4-rotor lift tests.

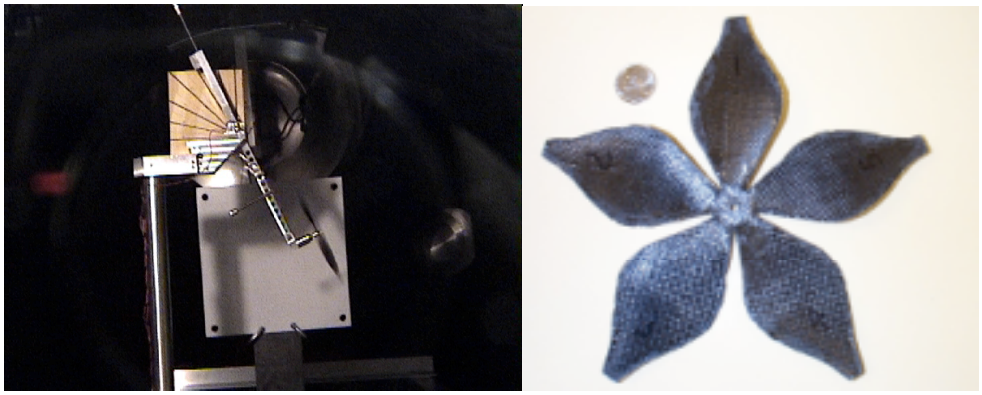

Figure 13. Rotor and experimental test set-up at JPL for miniature Mars rotorcraft.